Electronic Supplementary Material (ESI) for Soft Matter.

Supporting Information

Optically Tunable Chiral Nematic Mesoporous Cellulose Films

*Maik Schlesinger, Wadood Y. Hamad and Mark J. MacLachlan**

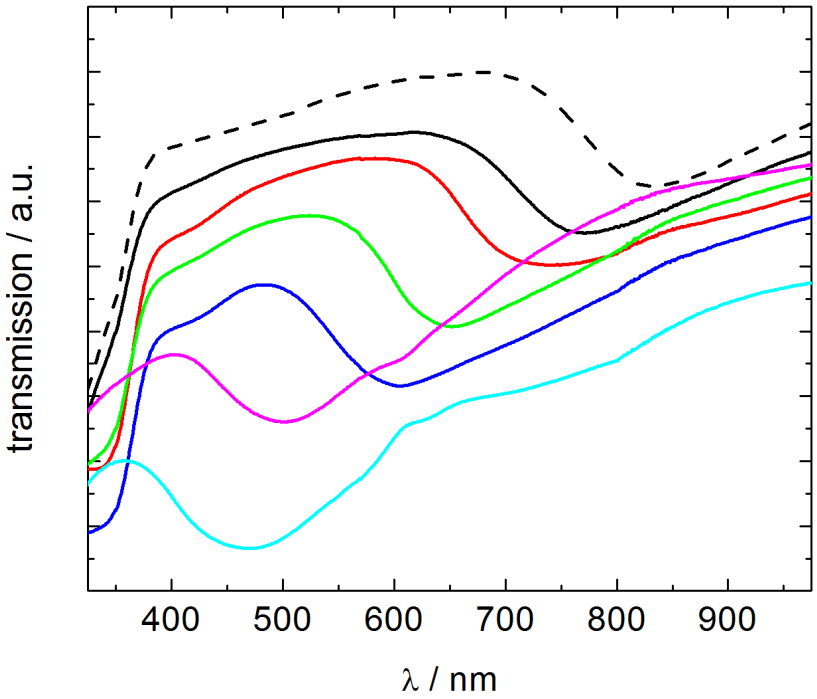

Figure S1. UV/Vis spectra of time-dependent treatment of **CNC/Si-1** (black, dashed) with a 4.2 wt% aqueous lithium hydroxide solution (black: 15 min; red: 30 min; green: 1 h; blue: 2 h; magenta: 48 h) and hydrofluoric acid (cyan: 15 min).

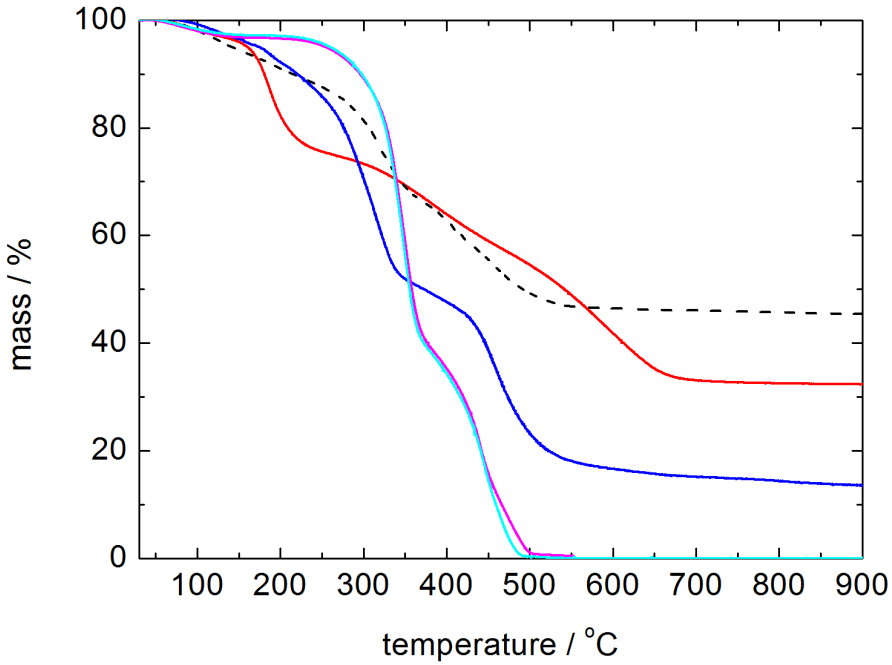

Figure S2. TGA curves (air, 10 °C min^{-1}) of **CNC/Si-1** (black, dashed) after treatment with a 4.2 wt% aqueous lithium hydroxide solution (red: 30 min; blue: 2 h; magenta: 48 h) and hydrofluoric acid (cyan: 15 min).

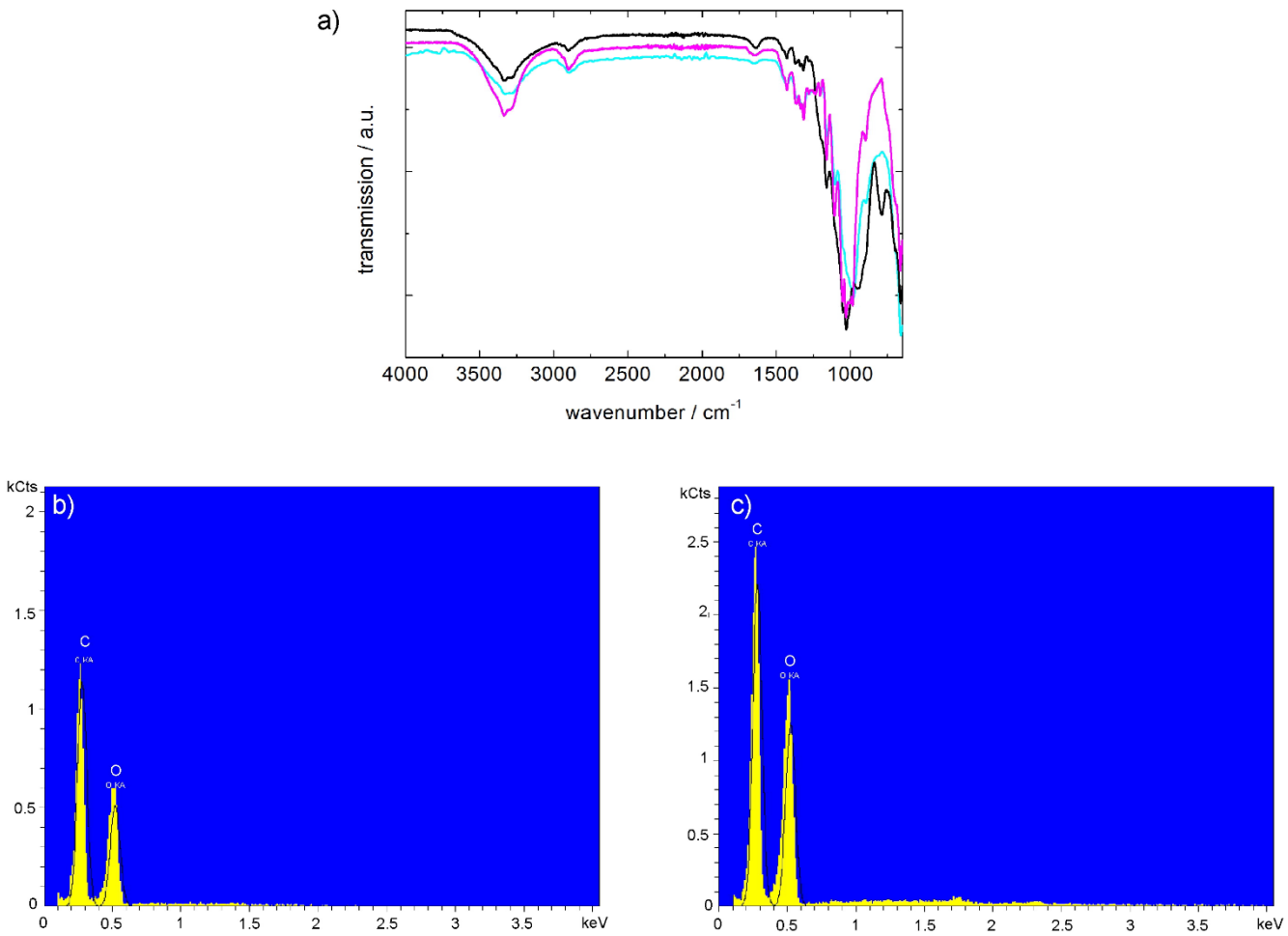

Figure S3. a) IR spectra of **CNC/Si-1** (black), **CNC/Si-1(48h)** (magenta) and **CNC/Si-1-HF** (cyan); b) EDX spectrum of **CNC/Si-1(48h)**; c) EDX spectrum of **CNC/Si-1-HF**.

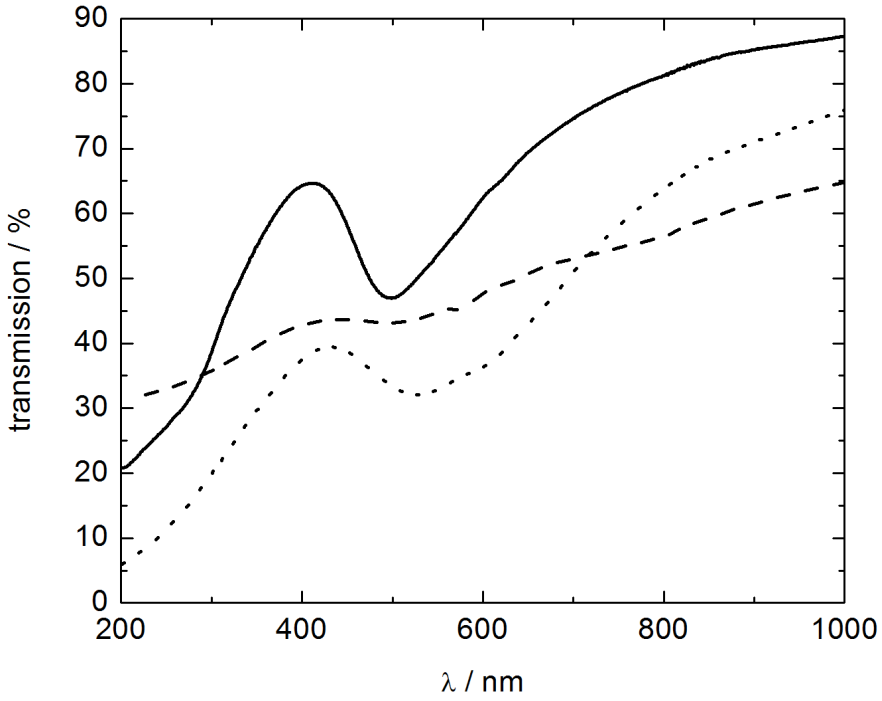

Figure S4. UV/Vis spectra of **CNC/Si** after treatment with 1.825 M aqueous solutions of lithium hydroxide (solid line, UV/Vis reflection band: 498 nm), sodium hydroxide (dashed line, UV/Vis reflection band: 502 nm) and potassium hydroxide (dotted line, UV/Vis reflection band: 528 nm) for 48 h.

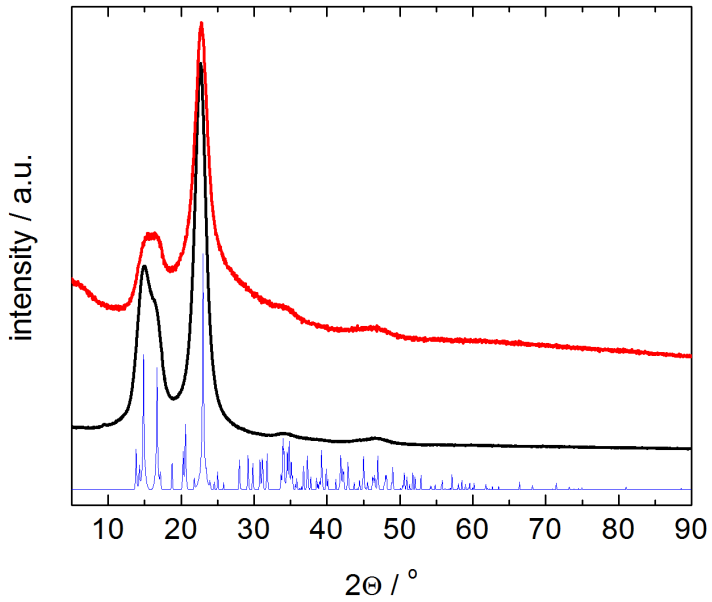

Figure S5. PXRD patterns of **CNC** (black), **CNC/Si-1** (red) and cellulose I*β* (calculated from CCDC 810597).

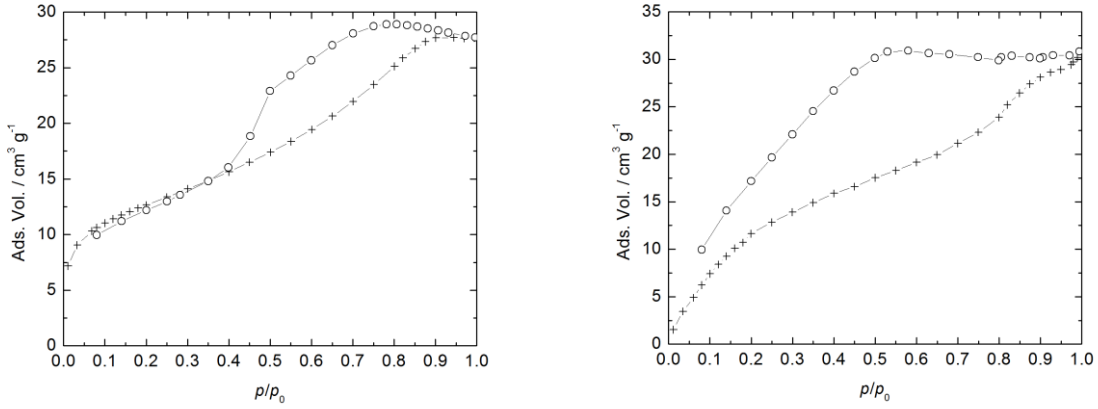

Figure S6. N_2 adsorption isotherms of **CNC/Si-1(48h)** (left) and **CNC/Si-1-HF** (right) after drying under ambient conditions.

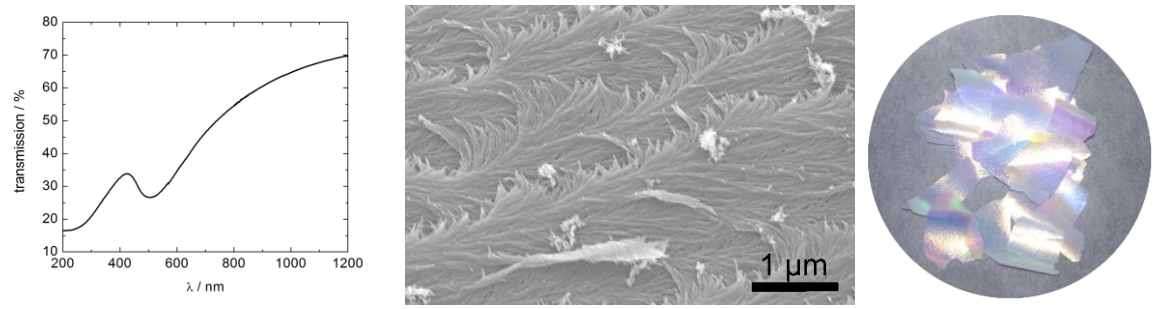

Figure S7. UV/Vis spectrum (left), SEM image (middle) and photograph (right) of **CNC/Si-1(48h)** after sc-CO_2 drying.

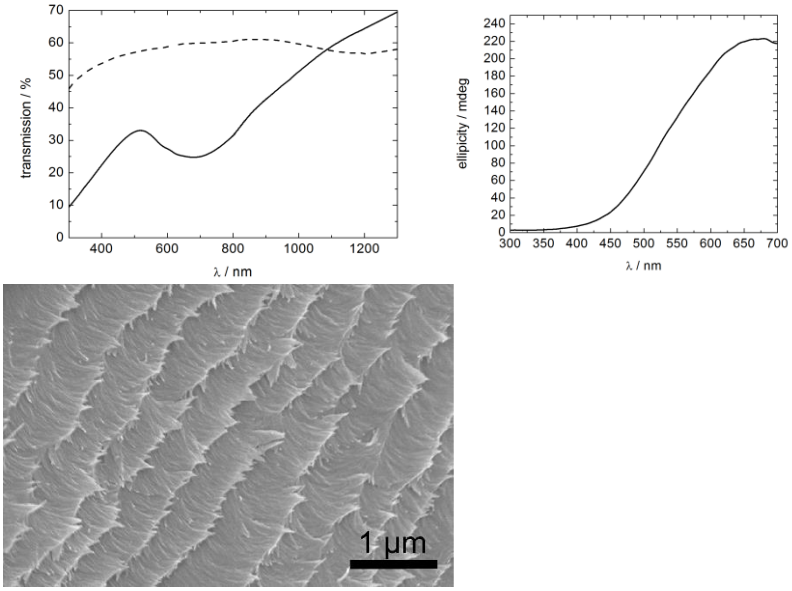

Figure S8. UV/Vis spectra (left) of **CNC/Si-2** (dashed line) and **CNC/Si-2(48h)** (solid line); CD spectra (middle) and SEM image (right) of **CNC/Si-2(48h)**.

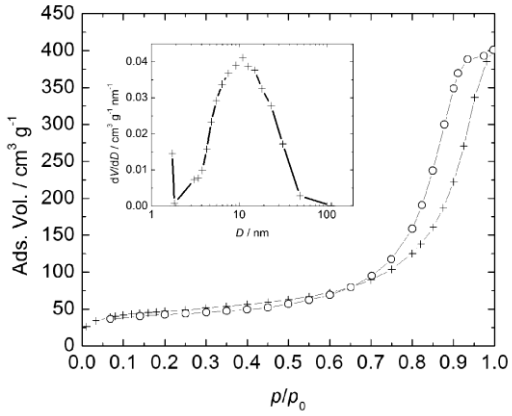

Figure S9. N_2 adsorption isotherm and BJH pore-size distribution (inset) of **CNC/Si-2(48h)** after sc-CO_2 drying.

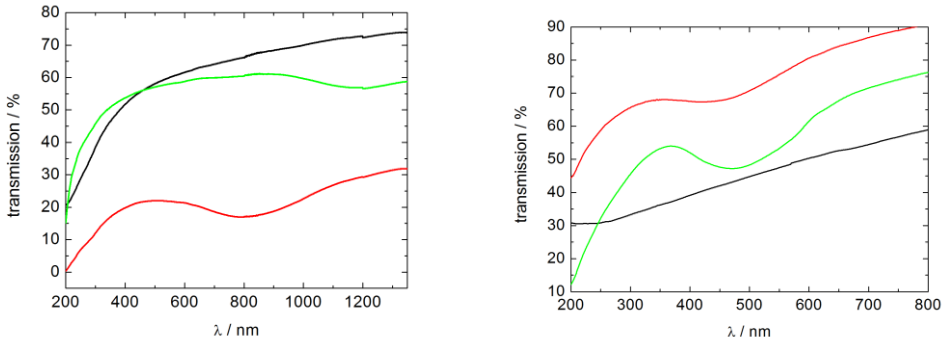

Figure S10. UV/Vis spectra of **CNC/Si-PS** (left, green line), **CNC/Si-CA** (left, red line), **CNC/Si-Al** (left, black line), **CNMC-PS** (right, green line), **CNMC-CA** (right, red line) and **CNMC-Al** (right, black line).

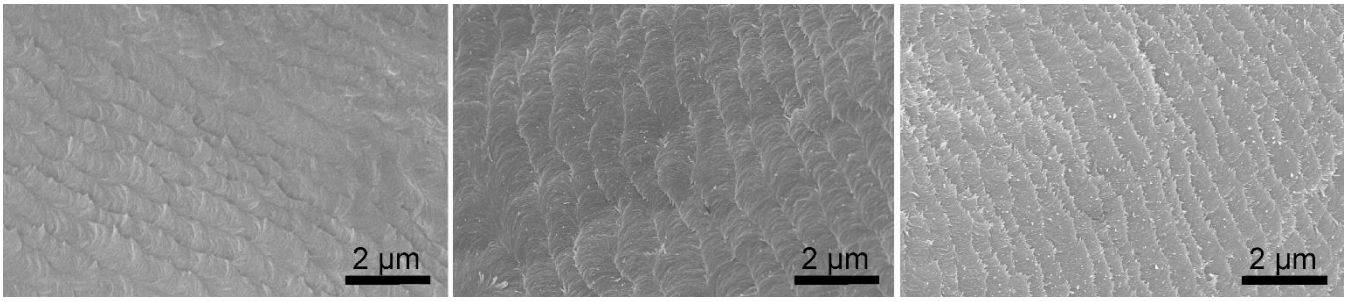

Figure S11. SEM images of **CNMC-PS** (left), **CNMC-CA** (middle) and **CNMC-Al** (right).

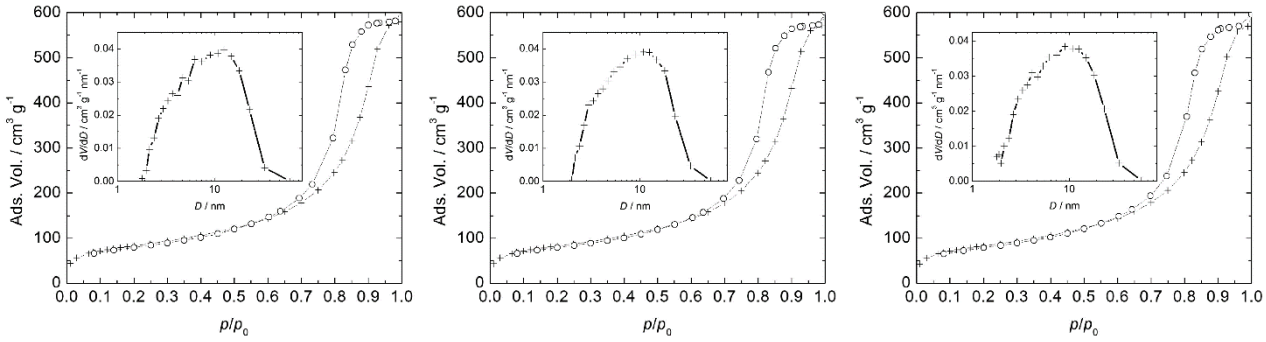

Figure S12. N_2 adsorption isotherm and BJH pore-size distribution (inset) of **CNMC-PS** (left), **CNMC-CA** (middle) and **CNMC-Al** (right).

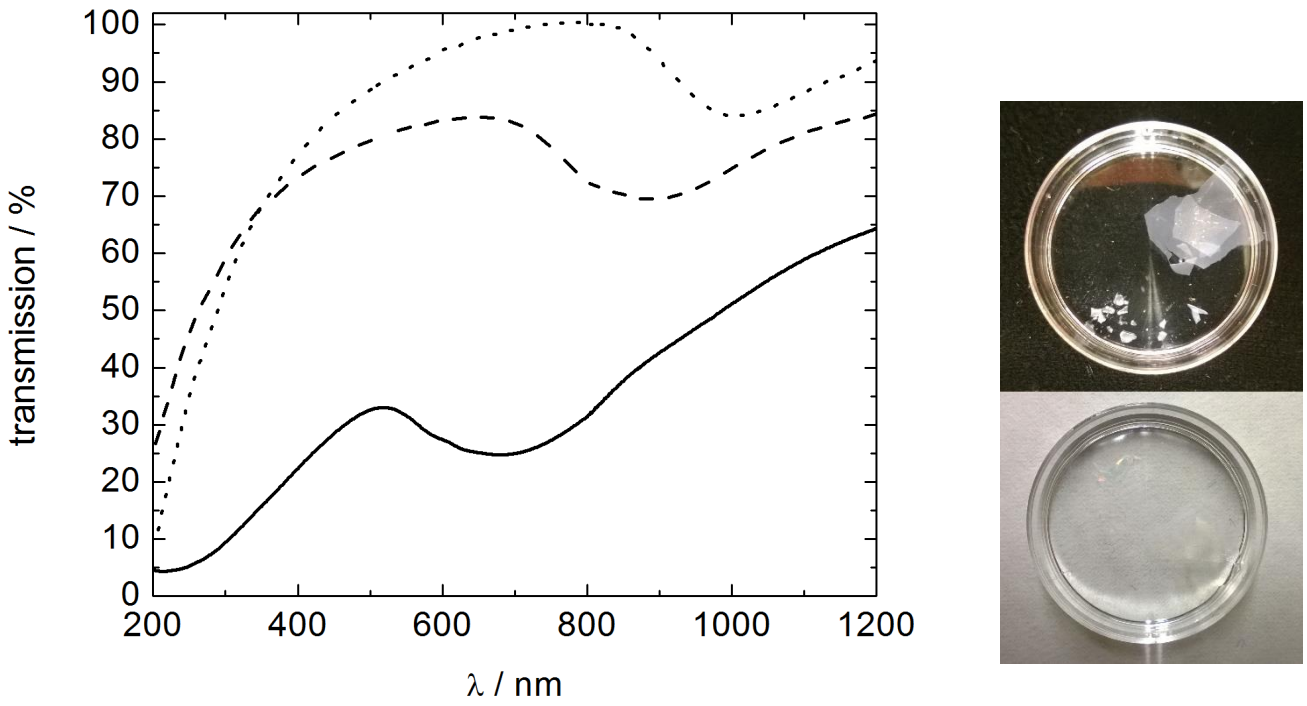

Figure S13. UV/Vis spectra (left) of dry **CNC/Si-2(48h)** (solid line) and after soaking in ethanol (dashed line) or water (dotted line). Photographs (right) of **CNC/Si-2(48h)** after soaking in water.

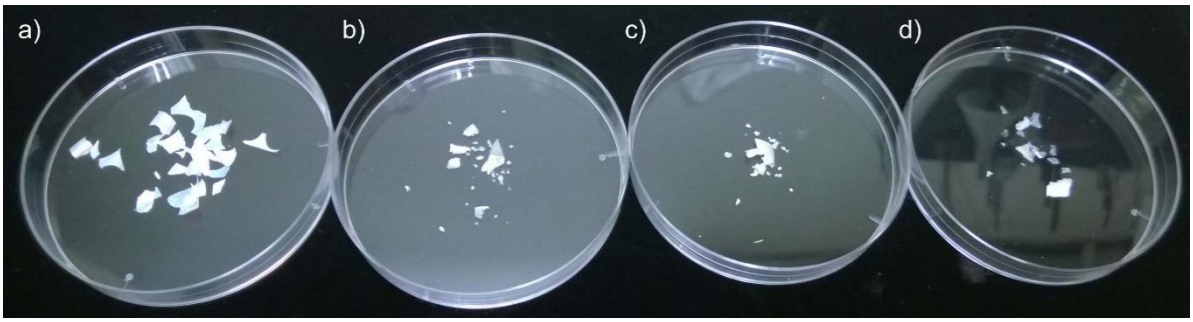

Figure S14. Photographs of unloaded CMNC (a), **CNMC-Au-5** (b), **CNMC-Au-10** (c) and **CNMC-Au-100** (d).

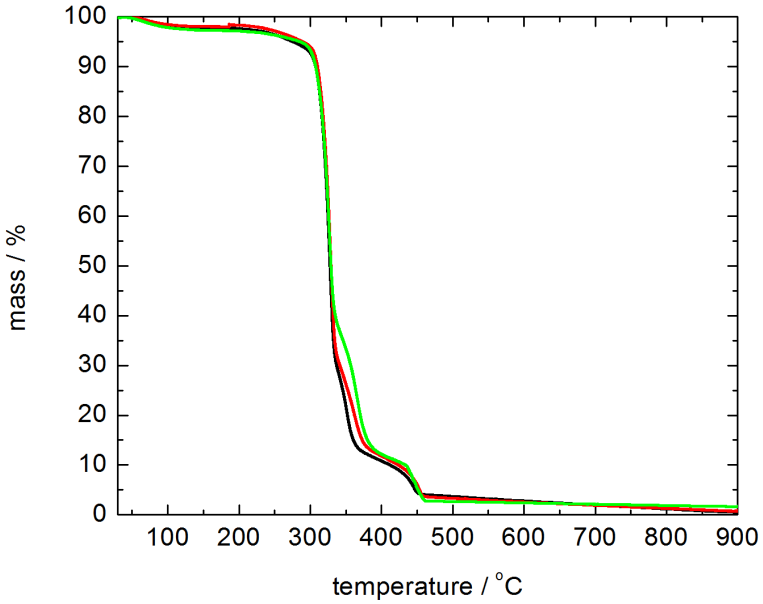

Figure S15. Thermogravimetric analyses of **CNMC-Au-5** (black line), **CNMC-Au-10** (red line) and **CNMC-Au-100** (green line).

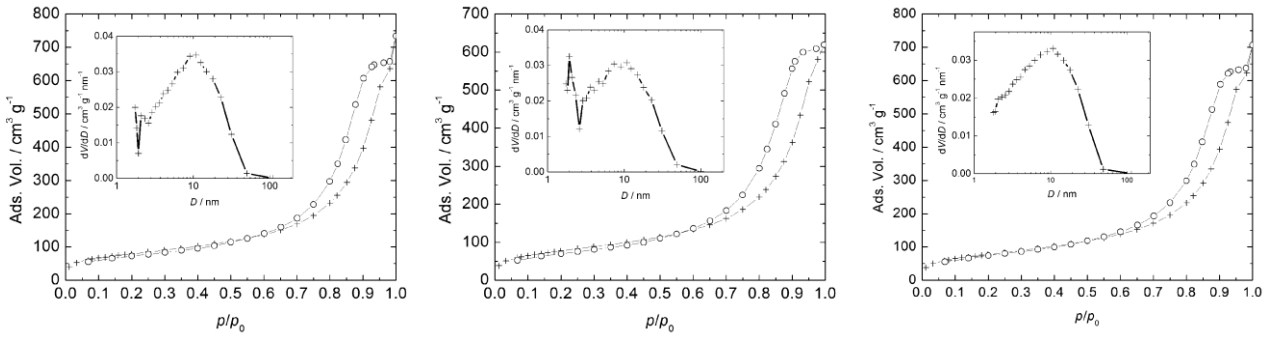

Figure S16. N_2 adsorption isotherms and BJH pore-size distributions (inset) of **CNMC-Au-5** (left), **CNMC-Au-10** (middle) and **CNMC-Au-100** (right) after sc-CO_2 drying.

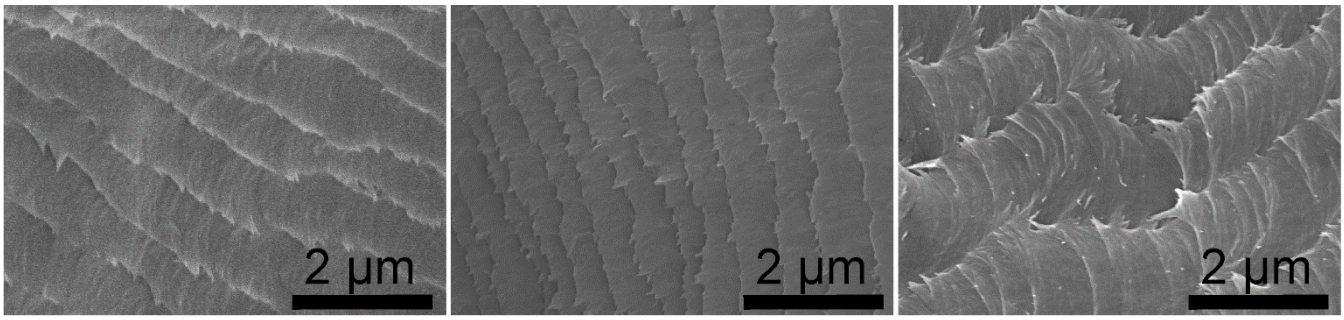

Figure S17. SEM images of **CNMC-Au-5** (left), **CNMC-Au-10** (middle) and **CNMC-Au-100** (right).

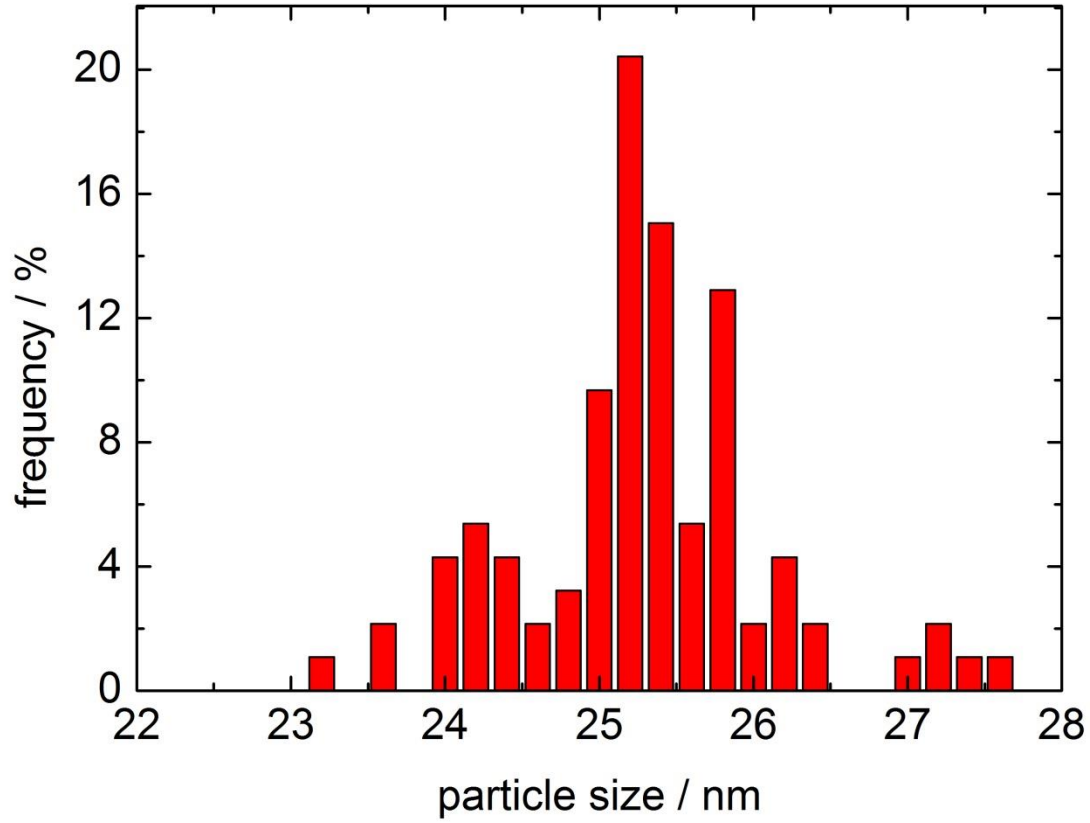

Figure S18. Particle size distribution for **CNMC-Au-10**. The mean particle size determined from counting 93 nanoparticles is 25.3 ± 0.8 nm.

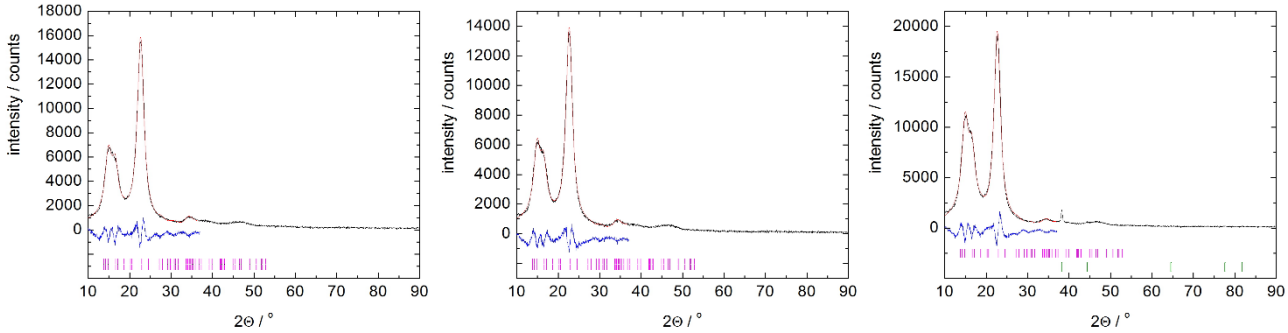

Figure S19. Powder X-ray diffraction patterns (black lines) of **CNMC-Au-5** (left), **CNMC-Au-10** (middle) and **CNMC-Au-100** (right). The diffraction patterns are resolved between 10° - 37° 2θ into crystalline peaks and amorphous background (red lines; this region was used as there is no interference with the diffraction peaks of Au NPs (green; PDF 03-065-2870)). The refinement was done using the Ruland-Rietveld analytical approach of the crystal structure of cellulose I*β* (CCDC 810597; magenta). The degree of crystallinity was determined to be ~86% (**MPC-Au-5**), ~80% (**MPC-Au-10**) and ~84% (**MPC-Au-100**).

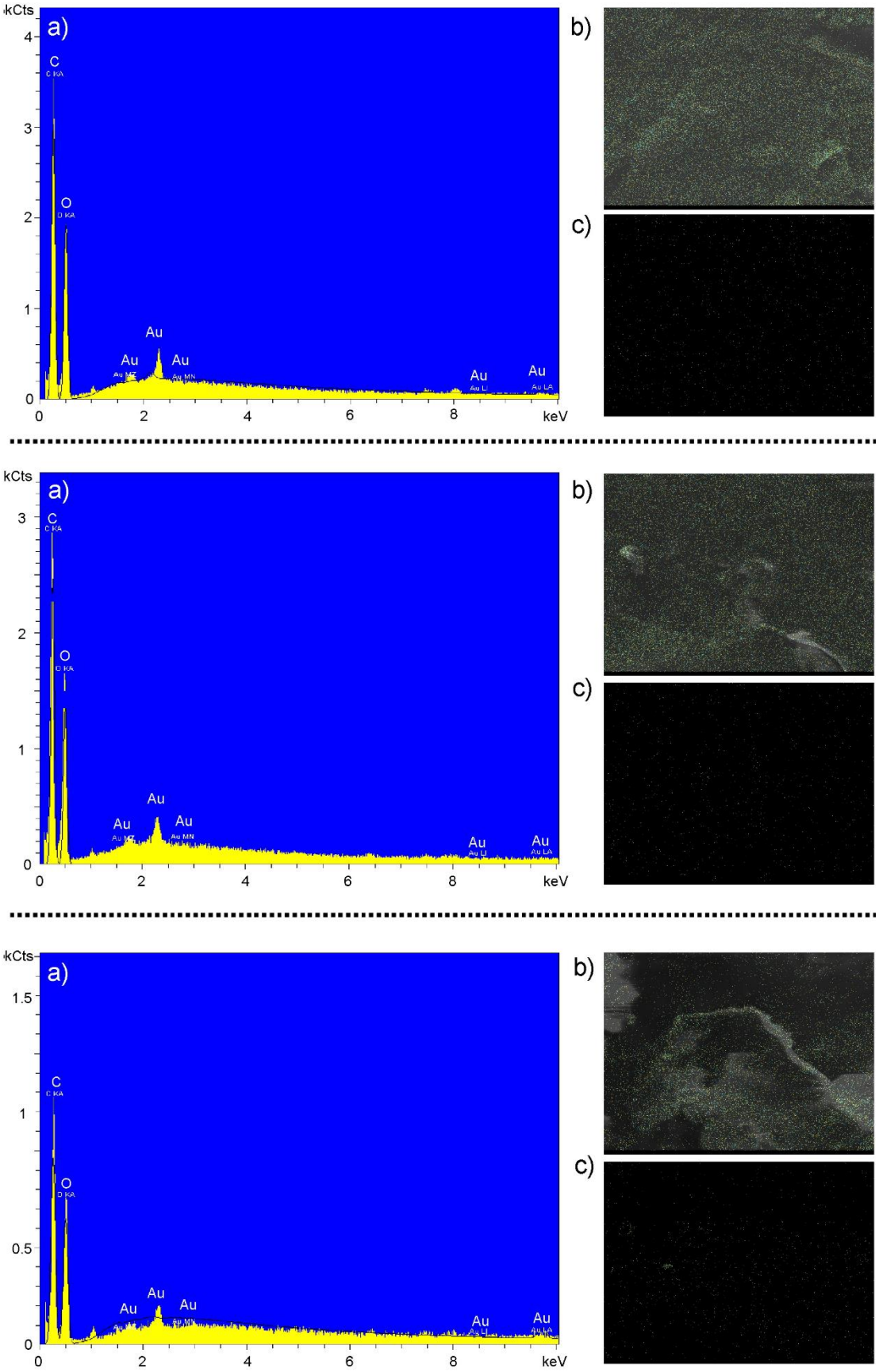

Figure S20. EDX spectra (a), EDX mapping combined with SEM image (b) and EDX mapping for gold (c) of **CNMC-Au-5** (top), **CNMC-Au-10** (middle) and **CNMC-Au-100** (bottom).

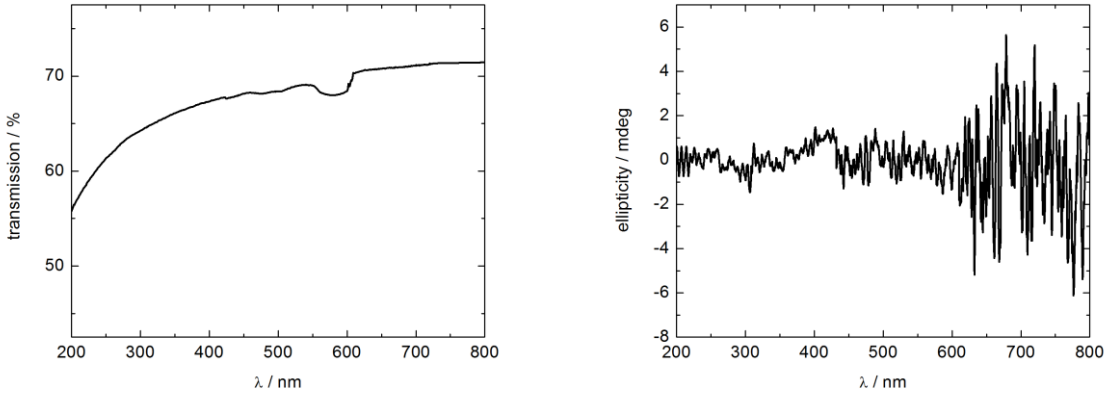

Figure S21. UV/Vis (left) and CD (right) spectra of gold loaded (100 mM) achiral nematic mesoporous cellulose.

Table S1. BET surface areas, pore volumes and BJH pore-size distributions of **CNMC-Au-5**, **CNMC-Au-10** and **CNMC-Au-100**

sample	BET-A_o ($m^2\ g^{-1}$)	Pore volume ($cm^3\ g^{-1}$)	BJH pore-width (nm)
CNMC-Au-5	284	1.13	14.0
CNMC-Au-10	279	0.96	12.3
CNMC-Au-100	281	1.09	13.2